Spin-liquid dynamics of pyrochlore magnets $Gd_2Ti_2O_7$ and $Gd_2Sn_2O_7$

S. S. Sosin, L. A. Prozorova, A. I. Smirnov

P. L. Kapitza Institute for Physical Problems RAS, 119334 Moscow, Russia

P. Bonville and G. Jasmin - Le Bras

Commissariat à l'Énergie Atomique, Centre de Saclay, DSM/SPEC, 91191 Gif sur Yvette, France

O. A. Petrenko

Department of Physics, University of Warwick, Coventry CV4 7AL, UK

(Dated: February 2, 2008)

The spin-liquid phase of two highly frustrated pyrochlore magnets $Gd_2Ti_2O_7$ and $Gd_2Sn_2O_7$ is probed using electron spin resonance in the temperature range 1.3 – 30 K. The deviation of the absorption line from the paramagnetic position $\nu = \gamma H$ observed in both compounds below the Curie-Weiss temperature $\Theta_{CW} \simeq 10$ K, suggests an opening up of a gap in the excitation spectra. On cooling to 1.3 K (which is above the ordering transition $T_N \simeq 1.0$ K) the resonance spectrum is transformed into a wide band of excitations with the gap amounting to $\Delta \simeq 26$ GHz (1.2 K) in $Gd_2Ti_2O_7$ and 18 GHz (0.8 K) in $Gd_2Sn_2O_7$. The gaps increase linearly with the external magnetic field. For $Gd_2Ti_2O_7$ this branch co-exists with an additional nearly paramagnetic line absent in $Gd_2Sn_2O_7$. These low lying excitations with gaps, which are preformed in the spin-liquid state, may be interpreted as collective spin modes split by the single-ion anisotropy.

PACS numbers: 75.30.Sg, 75.50.Ee, 75.30.Kz.

I. INTRODUCTION

The properties of a Heisenberg antiferromagnet on a pyrochlore lattice are determined to a great extent by the high degree of frustration of the nearest-neighbor exchange interaction. The minimum of the exchange energy can be achieved in an infinite number of degenerate states with different spin configurations. A classical consideration of the fluctuations between the states[1] and quantum calculations of a spin correlation function[2] show that the system should remain in a collective paramagnetic state with short-range spin correlations at any non-zero temperature. In real systems, the interplay of weaker contributions such as the dipolar interaction, single-ion anisotropy and next-nearest-neighbor exchange can lift the macroscopic degeneracy of the ground state driving the system into a particular ordered state. This principle reveals itself as a delay in the magnetic ordering transition to temperatures well below the Curie-Weiss temperature. This type of behavior is demonstrated by two related compounds $Gd_2Ti_2O_7$ and $Gd_2Sn_2O_7$ with spin $S = 7/2$ and zero orbital momentum $L = 0$ for the Gd^{3+} ions. Both systems have a Curie-Weiss temperature of about 10 K while the magnetic ordering develops only below 1.0 K.[3,4,5]

The strong degeneracy of the ground state implies the presence of a macroscopic number (half of the number of magnetic ions for a pyrochlore lattice) of local soft modes which should acquire the gaps and dispersion due to weak interactions. Intensive theoretical studies were performed for various combinations of interactions.[6,7,8,9] For example, the complex 4k-structure described by $k = (1/2, 1/2, 1/2)$ and equivalent wave-vectors which was proposed for $Gd_2Ti_2O_7$ by Stewart *et al.*,[10] can be stabilized under the combined influence of the dipolar interaction and one of the next-nearest neighbor exchanges. A large number of nonfreezing degrees of freedom in the correlated state immediately leads to an enhanced magnetocaloric effect in the vicinity of the saturation field, where the system undergoes a transition into a single spin-polarized state and all the modes acquire a Zeeman gap.[11] This effect was seen in an adiabatic demagnetization experiment.[12] However, a comprehensive study of this type of excitations has yet to be performed. Since inelastic neutron scattering experiments in these compounds are hindered by the large absorption cross-section of Gd nuclei, the electron-spin resonance technique remains the most suitable microscopic probe of these excitations.

Our recent works on the magnetic resonance in $Gd_2Ti_2O_7$ (Ref. 13) and in $Gd_2Sn_2O_7$ (Ref. 14) were mainly devoted to the study of the ordered states, while the spin-liquid phase has not been investigated in details. At low temperature, the systems were shown to have a regular resonance spectra, where some of the resonance lines could be identified and described theoretically as quasi-local modes. An early high temperature ESR work[15] reported an unusual resonance behavior in $Gd_2Ti_2O_7$, suggesting it is highly anisotropic (contrary to other experiments). In addition, the influence of the crystal field was studied by electron paramagnetic resonance of Gd^{3+} ions placed into the nonmagnetic $Y_2Ti_2O_7$ and $Y_2Sn_2O_7$ matrices.[16,17] The energy of the effective single ion anisotropy of the form $D\hat{S}_z^2$, arising from mixing with excited $L \neq 0$ Gd^{3+} levels, amounts to $D = 0.2$ K for the titanate and 0.14 K for the stannate, which is comparable to the nearest-neighbor exchange integral $J \simeq 0.3$ K, but is still far beyond the values

necessary to interpret the anisotropic effects described in Ref. 15. This discrepancy served as an additional motivation for the present ESR study.

This paper describes in detail the resonance properties of $Gd_2Ti_2O_7$ and $Gd_2Sn_2O_7$ in the spin-liquid phase (above $T_N \simeq 1.0$ K). We have studied several single crystal and powder samples over a wide frequency range. The distinctive gap in the excitation spectrum of the ordered phases is shown to develop above the ordering transition with the value $\Delta \approx 1.2$ K and 0.8 K for $Gd_2Ti_2O_7$ and $Gd_2Sn_2O_7$ respectively. This gap increases as a linear function of the external field independently of its orientation with respect to the crystal axes. We also found a new type of excitations coupled with the microwave field polarized along the external magnetic field. The strong orientational dependences previously reported in Ref. 15 are attributed to electrodynamic resonances in the finite size samples with large magnetic permeability.

II. EXPERIMENTAL DETAILS AND RESULTS

A. Sample preparation and experimental techniques

The single crystal of $Gd_2Ti_2O_7$ was grown by the floating zone technique described in Ref. 18. Samples of the same series were previously used to obtain the magnetic phase diagram[19] and in the investigation of the enhanced magnetocaloric effect,[12] as well as for previous low temperature magnetic resonance studies.[13] Two plate-shaped samples of different sizes were cut from the original single crystal: a large sample (#1) with the dimensions $1 \times 1 \times 0.2$ mm^3 (about 1 mg), and a small sample (#2) of approximately $0.5 \times 0.5 \times 0.1$ mm^3 (0.15 mg). The samples were cut so that the plane of the plate coincided with the (111) plane of the crystal lattice. The preparation procedure for powder samples is briefly outlined in Ref. 5. A small amount of powder (0.2 – 0.3 mg) was taken for each measurement.

We performed a series of ESR experiments in the frequency range 9 to 140 GHz using three wideband transmission-type spectrometers with rectangular and cylindrical cavities of different sizes. Samples were glued inside the cavity either on one of its walls or (for single crystal plates) onto a small worm-wheel used to rotate the sample from outside the spectrometer. The cavity was inside the vacuum cell filled with Helium heat exchange gas, immersed into liquid ^{4}He and supplied with a heater and thermometer allowing a regulation of the temperature between 4.2 and 100 K. Temperatures below 4.2 K (down to the minimum experimental temperature 1.3 K) were achieved and regulated by pumping the helium bath. A magnetic field of up to 80 kOe was generated by a cryomagnet. The resonance spectra were obtained by recording the transmitted signal on the forward and backward field sweeps. The microwave power transmitted through the cavity with a sample inside is

determined by the relation:

$$P = P_0 \left(1 + 2\pi\chi''\alpha Q\right)^{-2}, \qquad (1)$$

where χ'' is the dynamic susceptibility of the sample, α is a filling factor, Q is a quality factor of the cavity, the latter two parameters being different for each cavity resonance mode. The dynamic susceptibility χ'' may correspond to one or several resonance lines with Lorentzian shape in angular velocity ω. In case of a linear relation between ω and the applied magnetic field, H, each of the lines can be expressed in the following form:

$$\chi'' = \frac{A}{\left(1 + \frac{(H - H_{\text{res}})^2}{\Delta H^2}\right)} + \frac{A}{\left(1 + \frac{(H + H_{\text{res}})^2}{\Delta H^2}\right)}, \qquad (2)$$

where H_{res} and ΔH are the position and the half-linewidth of the line respectively, $(H \mp H_{\text{res}})$ originates from the decomposition of the linear polarization of a microwave field into counterclockwise and clockwise circular polarizations. Using expressions (1) and (2), one can fit the experimental absorption signals by the sets of parameters $W = \alpha Q A$ (the signal amplitude), H_{res} and ΔH. In the case of a single Lorentzian, the curve can be integrated with respect to the field in order to approximately relate these parameters to the static susceptibility $W \Delta H / H_{\text{res}} = \alpha Q \chi_{\text{st}}$. Firstly, this allows the temperature dependence of the static susceptibility to be obtained from the EPR data at a given frequency and secondly, it provides a reference for comparing signals obtained at different cavity modes with uncertain α and Q.

B. Magnetization of $Gd_2Ti_2O_7$ and $Gd_2Sn_2O_7$

The starting point of the experiment was to test the magnetization process in powder samples of both compounds under fields up to 140 kOe exceeding by a factor of 2 the transition into the saturated state. The isothermal magnetization curves were measured at $T = 1.75$ K in a commercial VSM magnetometer. They were carried out in a step mode, with a field increase rate of 5 kOe/min. The sample thermalization is provided by a continuous He gas flow. No hysteresis on the backward field sweep was observed. The saturation moment was found to be exactly 7.0 μ_B per Gd ion in $Gd_2Sn_2O_7$ and 6.9 μ_B per Gd ion in $Gd_2Ti_2O_7$. The magnetization curves are presented in Fig. 1, with their values scaled to the theoretical saturation moment $M_{\text{sat}} = g\mu_B S = 7\mu_B$. The initial part of both curves are linear in a rather wide field range (the corresponding fits are shown in Fig. 1 by solid lines), which allows one to estimate the nearest-neighbour exchange constants. In a molecular field approximation, the relation $M/M_{\text{sat}} = g\mu_B H / 8JS$ gives the values of $J = 0.32$ K and 0.28 K respectively for $Gd_2Ti_2O_7$ and $Gd_2Sn_2O_7$. The saturation field can
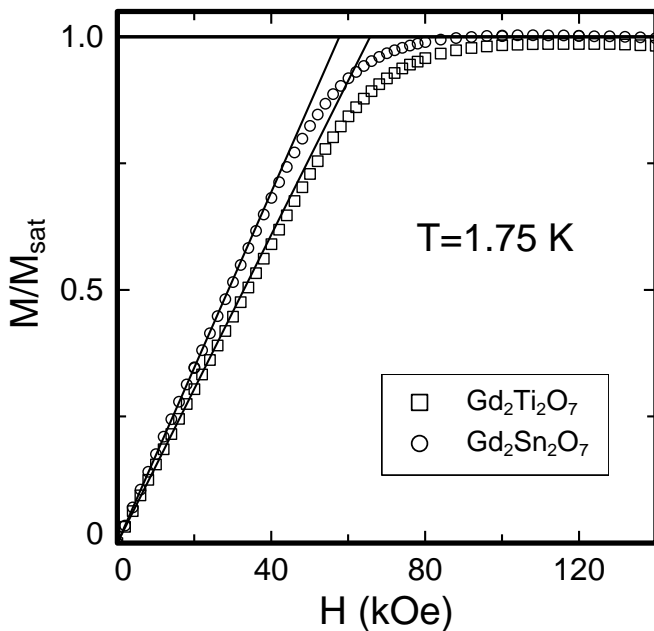
FIG. 1: Magnetization curves at $T = 1.75$ K scaled to the saturation magnetization $M_{\text{sat}} = g\mu_B S$ in $Gd_2Ti_2O_7$ ($\square$) and $Gd_2Sn_2O_7$ ($\bigcirc$) powder samples; solid lines are linear fits of the low field parts of the curves.

FIG. 2: (color online). The field dependence of the absorption in $Gd_2Ti_2O_7$ single crystals for $H \parallel [111]$ at the frequencies $\nu = 9.6$ GHz (sample #1, left panel), $\nu = 36.1$ GHz (sample #1, middle panel) and $\nu = 69.6$ GHz (sample #2, right panel). Solid lines are two-component Lorentzian fits as described in the text, the dashed and dashed-dotted lines show the Line I and Line II of the spectrum separately; out-of-curve points are DPPH labels used as a reference.

be also estimated by extrapolating these linear fits to $M = M_{\text{sat}}$ which yields $H_{\text{sat}} = 66$ kOe and 58 kOe. The result for $Gd_2Ti_2O_7$ exceeds by 10% the previously reported value of 59-61 kOe measured by ESR in the ordered phase for different orientations of the magnetic field.[13] A saturation field of 60 kOe was also obtained from pulse field magnetization measurements at $T = 0.3$ K,[20] so our extrapolation procedure with the data obtained at the temperature above the ordering transition gives an overestimate for the values of H_{sat} as well as for the exchange constants J.

One should mention that because of the large susceptibility, a correction to the internal magnetic field due to demagnetization effects in $Gd_2Ti_2O_7$ single crystal samples amounts to 10% for the field oriented perpendicular to the sample plates. Hereafter, we shall present the magnetic field as the internal field, i.e the one corrected for the demagnetization effect (using the above curves as well as data taken from Ref. 5).

C.   Electron spin resonance spectrum of $Gd_2Ti_2O_7$

In the main part of the present work we studied the temperature evolution of the resonance absorption in $Gd_2Ti_2O_7$ and $Gd_2Sn_2O_7$ samples at various microwave frequencies. The experimental results for the magnetic field applied parallel to [111] axis of a single crystal sample of $Gd_2Ti_2O_7$ are summarized in Fig. 2. The left, middle and right panels show the absorption curves recorded at the lowest, intermediate and high frequen-
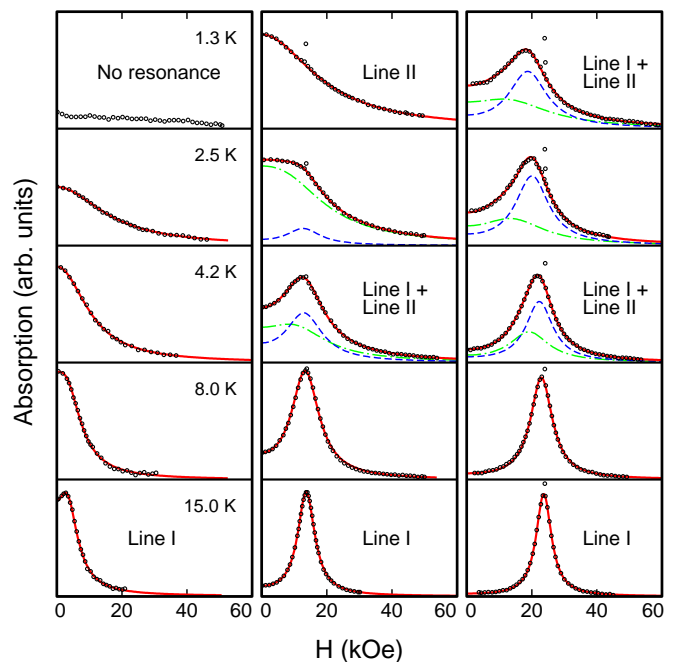
cies of 9.6 GHz, 36.1 GHz and 69.6 GHz respectively. At temperatures above the Curie-Weiss temperature ($T > \Theta = 10$ K) a single resonance line is observed over the whole frequency range. The best fits of these curves using a single Lorentzian form (2) are shown in Fig. 2 by the solid lines. The corresponding fitting parameters H_{res}, ΔH and $W\Delta H$ are analyzed in Figures 3,9. The resonance fields at all frequencies correspond to a paramagnetic g-factor equal to 2.0 for all orientations of the magnetic field (the dashed line on the upper panel of Fig. 9). This picture remains qualitatively the same at intermediate temperatures $T \sim \Theta$, with all the lines broadened and amplified. This behavior is typical for a concentrated paramagnet at high temperature, where the different spectral lines (split due to anisotropic effects) are narrowed into a single line due to the exchange interaction.

On decreasing the temperature further, the resonance lines continue to broaden and start to shift to lower fields. At the lowest frequency $\nu = 9.6$ GHz the line moves to zero field by $T = 4.2$ K and then decreases in amplitude and disappears completely at $T = 1.3$ K (see left panel of Fig. 2). This indicates that no observable (excited by the microwave field) resonance modes with energies below 10 GHz are left in the vicinity of the ordering transition at $T \geq T_{N1} = 1.0$ K. For frequencies below 30 GHz this
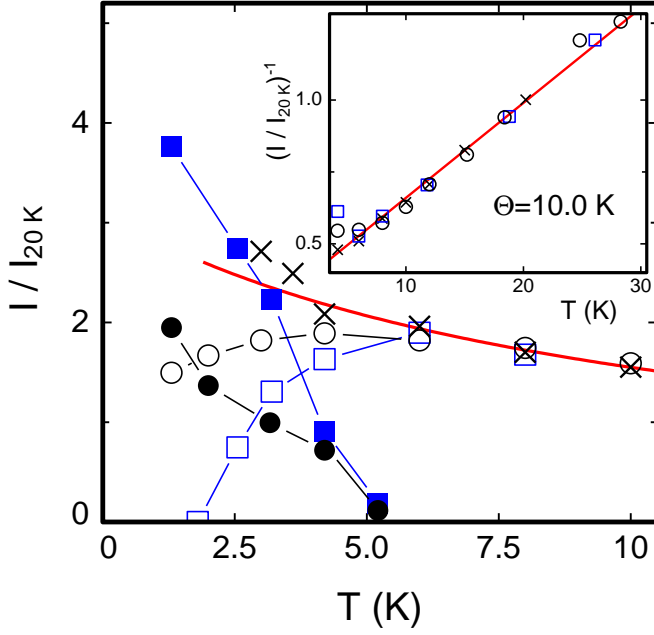
FIG. 3: (color online). The temperature dependence of the integrated intensity $I = W\Delta H$ of two resonance lines determined at various frequencies from fitting the transmitted signal by a single or double Lorentzian form (as described in the text) and scaled to the value obtained for 20 K; $\times$ – $\nu = 9.6$ GHz (Line I), $\square$ and $\blacksquare$ – 36.1 GHz, $\circ$ and $\bullet$ – 69.6 GHz (respectively Lines I and II). The inset represents the inverse values of the integrated intensity in the whole temperature range, the solid line is a paramagnetic fit with the Curie-Weiss temperature $\Theta = 10$ K.

tendency is preserved so that one can trace the gradual shift of the resonance line towards zero field on cooling until some temperature after which it is replaced by a broad line with a maximum absorption at $H = 0$. Fig. 3 shows the integrated intensity scaled to the intensity at $T = 20$ K. Down to approximately 2.5–3.0 K it obeys the Curie-Weiss law $\chi \sim 1/(T+\Theta)$ with $\Theta = 10$ K (solid line on Fig. 3) in accordance with previous magnetization measurements.[5,7]

A different behavior is observed at higher frequencies of 36.1 and 69.6 GHz. Below 4-6 K the resonance spectra cannot be fitted by a single Lorentzian line. An improvement is achieved by adding a second absorption, also with Lorentzian shape (the middle and right panels of Fig. 2). One of these lines remains around the paramagnetic position (Line I) while the second one shifts to smaller fields similarly to the previously described behavior at lower frequencies (Line II). At $\nu = 36.1$ GHz the intensity of the Line I rapidly decreases (as shown by open squares in the Fig. 3) while the intensity of the Line II increases (closed squares) and finally becomes the only resonance response of the sample at $T = 1.3$ K. This response has properties that are significantly different from those of the paramagnetic signal. It is also observed at the frequency $\nu = 69.6$ GHz, although the intensity of the para-
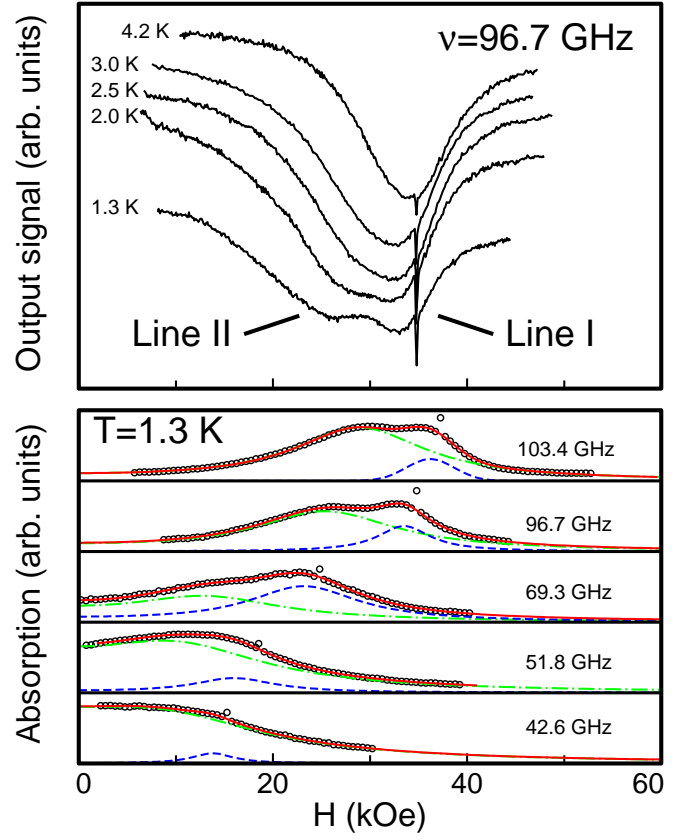

FIG. 4: (color online). The field dependence of the resonance absorption in $Gd_2Ti_2O_7$ powder sample for various temperatures at $\nu = 96.7$ GHz (upper panel) and at different frequencies at $T = 1.3$ K (lower panel); solid, dashed and dashed-dotted lines are the same as in Fig. 2, narrow signal and out-of-curve points are DPPH labels.

magnetic line does not drop to zero at the minimum temperature. Because of the large width of both lines at low temperatures ($\Delta H \simeq 8 - 10$ kOe and 15-20 kOe for the Line I and II respectively at $T = 1.3$ K), the dependence of the signal on the magnetic field direction cannot be traced.

On further increasing the measurement frequency the absorption of the single crystal samples is disrupted by a parasitic electrodynamic effect (described in details below in Subsection II F) and the measurements are only possible on powder samples. The typical temperature evolution of the signal from the powder sample obtained at $\nu = 96.7$ GHz is presented in the upper panel of Fig. 4. The single line positioned nearly to the paramagnetic DPPH label observed at $T = 4.2$ K is replaced by a double signal, with Line II increasing in intensity and shifting to smaller fields at lower temperatures. Since the linewidth of both signals tends to decrease at high frequencies (at larger values of the resonance fields) the splitting of the resonance absorption into two components becomes more prominent and easier to trace. The comparison of signal records taken at different frequen-
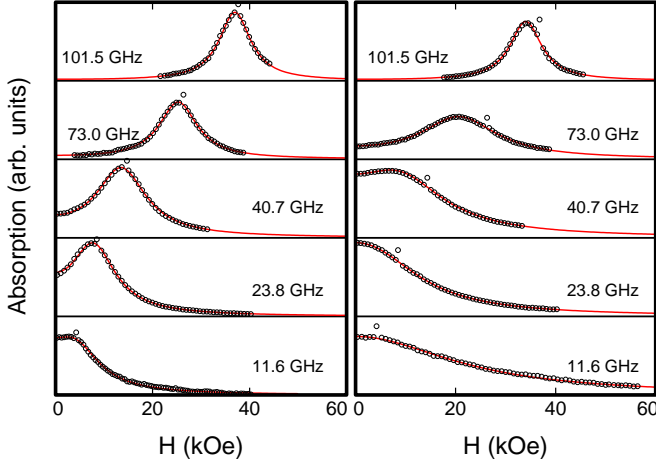
FIG. 5: (color online). The field dependence of the resonance absorption in $Gd_2Sn_2O_7$ powder sample for various frequencies at $T = 4.2$ K (left panel) and 1.3 K (right panel); solid lines are single Lorentzian fits to the experimental points.

cies (the lower panel of Fig. 4) illustrates this tendency and provides unambiguous proof of the resonance line doubling in $Gd_2Ti_2O_7$ at temperatures below 4 K.

D. Electron spin resonance spectrum of $Gd_2Sn_2O_7$

The absorption spectra of $Gd_2Sn_2O_7$ are presented in Fig. 5 for two temperatures: 4.2 K (in the left panel) and the minimum experimental temperature 1.3 K (right panel). A single resonance line observed at 4.2 K was found to gradually broaden and shift to smaller fields with no trace of splitting. The splitting is evidently absent even above 100 GHz, where the linewidth is small enough ($\Delta H \leq 5$ kOe) for the two components to be reliably resolved as it is the case for $Gd_2Ti_2O_7$ (see the previous Section).

E. Longitudinal microwave susceptibility

The results of the previous section were obtained for the microwave field h_{mw} polarized perpendicular to the external magnetic field. Such a polarization is typical for ESR experiments. The high frequency response of $Gd_2Ti_2O_7$ sample #2 was also studied in a "parallel" polarization of the microwave field for which the spin precession of the paramagnetic type cannot be excited. Instead, one can probe the longitudinal oscillations of the magnetic moment associated with the internal degrees of freedom of the correlated spin system. The microwave polarization for the TE_{01n} modes in the rectangular cavity can be selected by placing the sample either on the vertical centerline of the wide cavity wall ($h_{mw} \perp H$) or on its narrow wall ($h_{mw} \parallel H$). In both cases the polarization is almost perfect as the sample size is much smaller
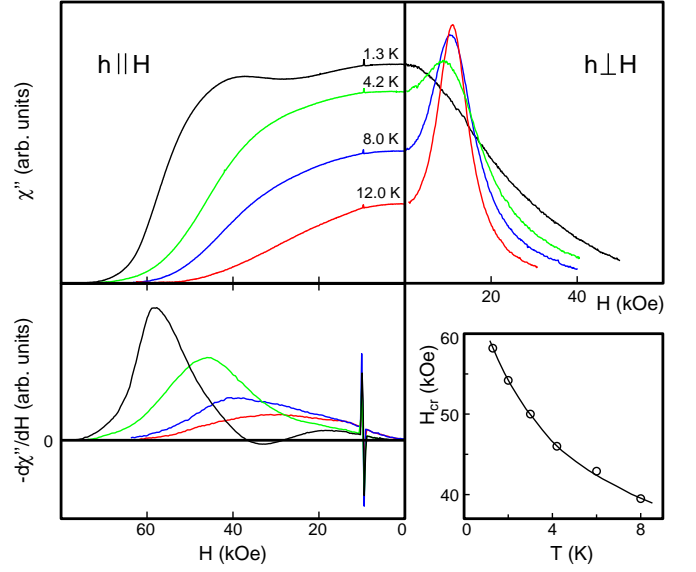

FIG. 6: (color online). Field dependence of the resonance absorption and its derivative (upper and lower left panels respectively) at the frequency $\nu = 27.1$ GHz for the microwave field polarized along the direction of the external magnetic field, and the corresponding data for the perpendicular microwave field polarization (upper right panel). Lower right corner inset shows the temperature evolution of the crossover into the ground state with destroyed "soft modes"; the solid line is a guide to the eye.

than the dimensions of the cavity.

A comparison between the sample responses observed at a frequency $\nu = 27.1$ GHz for the two polarizations of the microwave field is presented in Fig. 6. The data for $h_{mw} \parallel H$ and $h_{mw} \perp H$ are rescaled to each other by the values of $\chi''(H = 0)$ obtained at $T = 12$ K. The field dependences of the sample absorption at different temperatures for $h_{mw} \parallel H$ are shown in the upper left panel. The high temperature curve ($T = 12$ K) at low fields shows an absorption with an amplitude corresponding to the wing of a Lorentzian resonance line of the form (2). The intensity of this signal is attenuated at fields comparable to the saturation field of an $S = 7/2$ paramagnet. The absorption for the perpendicular polarization shown on the upper right panel corresponds to a paramagnetic line with $g = 2.0$ that is well fitted by (2). On lowering the temperature the magnetic field required to suppress the longitudinal susceptibility of the system increases reaching 60 kOe at $T = 1.3$ K. This value exceeds by a factor of 10 the paramagnetic saturation field and corresponds to the transition of the exchange correlated structure into a fully polarized state. Roughly the same value 66 kOe was obtained from our magnetization measurements. The shift of the suppression field is illustrated on the lower left panel by the derivative of the absorption by magnetic field. The temperature dependence of the corresponding inflection points is shown on the lower right inset to Fig. 6. For the perpendicular polarization

(see the upper right panel) the perfect paramagnetic line developed at high temperatures is gradually transformed into a broad absorption with the maximum positioned at zero field (as described in previous sections). By comparing the $T = 1.3$ K curves for $h_{mw} \parallel H$ and $h_{mw} \perp H$ one can conclude that the strongly correlated disordered spin state in $Gd_2Ti_2O_7$ possesses low energy internal degrees of freedom amenable to the longitudinal microwave field. The absorption intensity is reduced by an external field applied perpendicular to the direction of the microwave field but is practically insensitive to the parallel magnetic field up to the crossover into the state where the collective degrees of freedom are destroyed by temperature and magnetic field. In the low temperature limit this crossover corresponds to the transition into the spin-polarized state in which the system cannot respond to the weak perturbation of the saturated magnetic moment.

F. Resonance "size effects"

The main features of the resonance spectra observed in $Gd_2Ti_2O_7$ single crystals are described in Sections II C and II E. Here we draw the attention to the unusual resonance behavior first reported in Ref. 15, which is also observed in our samples. At frequencies above 60 GHz the resonance line in the single crystal sample #1 appears to be split into two broad components, both having strong temperature and orientational dependences whose typical shape is shown in Fig. 7 for $\nu = 69.4$ GHz. The temperature evolution of the absorption persists over the whole temperature range until 30 K. The signal also varied strongly with a period of nearly $180°$ when rotating the sample inside the resonator (see Fig. 7, left panel). Such properties are usually indicative of systems with a strong uniaxial anisotropy, with a value much larger than the exchange interaction; this was indeed suggested in Ref. 15 to explain the results presented there. Nevertheless, this suggestion obviously contradicts all the other experimental data on the compound, which show the single-ion anisotropy constant does not exceed 0.2 K (see for example Ref. 16).

Our experiments show this problem can be eliminated by decreasing the size of the sample. Fig. 8 illustrates how the absorption signal is modified for sample #2 with linear dimensions of approximately one half of sample #1. The resonance absorption, measured at the same cavity frequency in order to avoid any influence of polarization effects, demonstrates dramatic changes in the response to the microwave field. Namely, the intense high field absorption with unusual temperature and orientational properties disappears and the resonance line acquires the shape described in the Section II C above (for comparison, see the corresponding curves on the lower and upper panels of Fig. 8 taken at $\nu = 69.4$ and 69.6 GHz respectively). On further increasing the frequency of the measurement the splitting reappears (see the curve at $\nu = 96.4$ GHz) revealing the same charac-
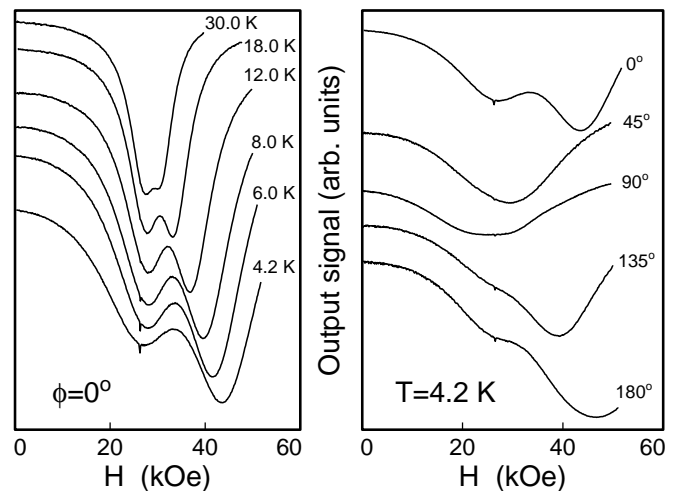

FIG. 7: The field dependences of the absorption at $\nu = 69.4$ GHz in the sample #1 recorded at different temperatures for $H \parallel [111]$ (left panel), and at $T = 4.2$ K for different sample orientations (right panel); narrow peaks at all curves is a paramagnetic DPPH label.
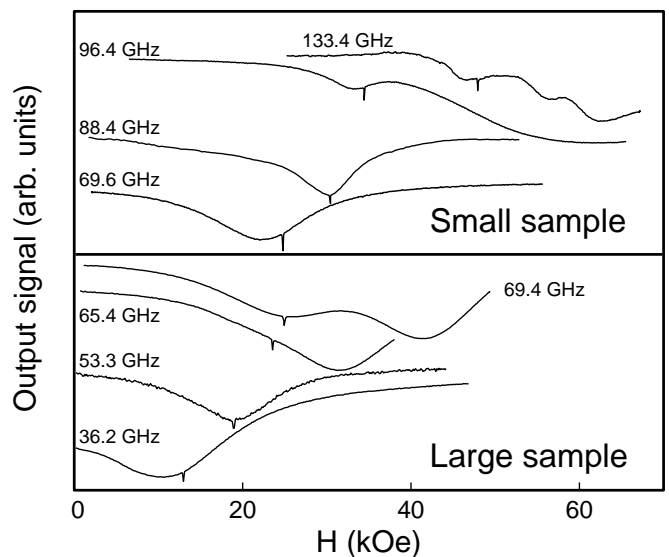

FIG. 8: The comparison of absorption spectra of the sample #1 (lower panel) and sample #2 (upper panel) taken at $T = 4.2$ K for several frequencies; the upper curve for the large sample and the lower curve for the small sample are obtained at the same frequency of the cylindrical cavity.

teristic features as a function of temperature and sample orientation.

We therefore suggest that this effect is associated not with the properties of a pyrochlore, but rather with the geometry of the sample, its large dielectric constant ε and its field dependent permeability μ. When one of the linear sample dimensions l roughly meets the condition

$$l \sim n \frac{\lambda}{2\sqrt{\varepsilon \mu}}, \qquad (3)$$

where λ is the electromagnetic wavelength in free space and n is an integer, an electrodynamic resonance takes place, with the sample playing the role of the resonator, and its absorption rises. The smaller the sample size l, the higher the boundary frequency for this effect to reveal itself. The value of $\mu' = 1 + 4\pi\chi'$ is enhanced in $Gd_2Ti_2O_7$ as a result of the large spin value of Gd and a relatively small saturation field of the magnetic structure. In addition, the field dependence of χ' has a singularity in the vicinity of the paramagnetic resonance field $\chi' \sim (H - H_{pm})/(1 + (H - H_{pm})^2/\Delta H^2)$ which can be responsible for meeting the resonance condition (3) twice (or more) during a field scan. One of these "resonance" fields is positioned near H_{pm} while the other should be shifted away from it. The value of this shift increases on lowering the temperature due to the increase of the singularity amplitude as was observed in our experiment. In the high frequency limit, the number of such electrodynamic modes grows, resulting in further splitting of the absorption line (see the 133.4 GHz curve in Fig. 8). Due to the coupling with the main cavity this signal should be sensitive to the orientation of the sample plate with respect to the distribution of the microwave field in the cavity, which explains the observed 180° periodic dependence. One should mention that the effect described above is only present for continuous samples. In order to extend the frequency range over which reliable results can be obtained, we used powder samples spread over the resonator wall in the shape of a thin rarefied film.

III. DISCUSSION AND CONCLUSIONS

We begin the analysis of the data for $Gd_2Ti_2O_7$ and $Gd_2Sn_2O_7$ described in the previous sections starting from the high temperature region $T \geq \Theta_{CW}$, where a single paramagnetic resonance line corresponding to an isotropic g-factor of 2.0 is observed in both systems (its frequency-field dependence is shown by dashed lines in Fig. 9). This line results from the exchange narrowing of a set of spectral components split by the single-ion anisotropy. The initial broadening of this line on decreasing the temperature down to $T \simeq \Theta_{CW}$ and its shift to smaller magnetic fields reflect the redistribution of spin sublevel populations. Such a behavior is common for concentrated paramagnets.

The single resonance line corresponding to the paramagnetic precession can be traced in the frequency range 9–100 GHz down to approximately 4–6 K. The temperature dependence of the intensity of this signal in $Gd_2Ti_2O_7$ single crystal obtained by integrating the Lorentzian line over a field scan (proportional to the static susceptibility of the sample) is nicely fitted by a Curie-Weiss law with
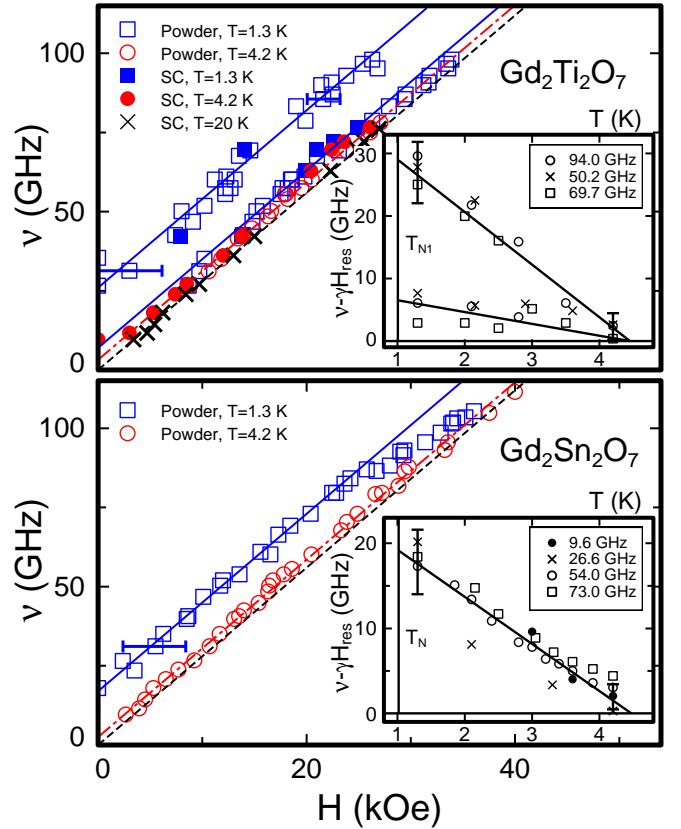

FIG. 9: (color online). The frequency-field diagram of the obtained ESR spectra. Upper panel – $Gd_2Ti_2O_7$ powder sample ($\square$ and $\bigcirc$) and single crystal with $H \parallel [111]$ ($\blacksquare$, $\bullet$ and $\times$) at different temperatures. Lines are $\nu = \Delta + \gamma H$ ($\gamma = g\mu_B/h$ with $g = 2.0$) fits to the data points: dashed, dashed-dotted and solid lines correspond to $T = 20$ K, 4.2 K and 1.3 K respectively with the gaps $\Delta = 0$ (a typical concentrated paramagnet), 3.5 GHz, 5 and 26 GHz. The inset represents the temperature dependence of the value $\nu - \gamma H_{res}$ for the two resonance modes at various frequencies. Lower panel – analogous results for the powder sample of $Gd_2Sn_2O_7$ at $T = 4.2$ K ($\bigcirc$) and 1.3 K ($\square$) described by gapped linear dependences with $\Delta = 2.5$ GHz (dashed-dotted line) and 18 GHz (solid line); the inset is the same as for the $Gd_2Ti_2O_7$ panel, but with the single resonance line. (Error bars on both panels correspond to $\Delta H/5$).

$\Theta \approx 10.0$ K (see the inset to Fig. 3) in agreement with previous susceptibility measurements.[3,5] The corresponding dependence for $Gd_2Sn_2O_7$ is traced in details only below 4.2 K. The resonance fields, H_{res}, at $T = 4.2$ K determined from Lorentzian fits at various frequencies shift from the paramagnetic positions by 1–2 kOe (as shown in the frequency-field diagram of Fig. 9) giving the first evidence of a gap opening. Within the experimental accuracy, the $\nu(H)$ curves in both compounds obey the linear law $\nu = \Delta + \gamma H$ ($\gamma = g\mu_B/h$) with the g-factor equal to 2.0 and $\Delta = 3.5$ GHz (0.17 K) and 2.5 GHz (0.12 K) for $Gd_2Ti_2O_7$ and $Gd_2Sn_2O_7$ respectively (best fits to the experimental points are plotted by dashed-dotted lines).

The further temperature evolution of the spectrum reveals the considerable differences between the two systems. Namely, the resonance absorption in $Gd_2Sn_2O_7$ always consists of a single line gradually shifting to lower fields. At $T = 1.3$ K it can be again described as a linear function in magnetic field with $g = 2.0$ and $\Delta = 18$ GHz (solid line in the lower panel of Fig. 9).

In contrast, the high temperature resonance line of $Gd_2Ti_2O_7$ is transformed into a double line spectrum below 4 K. The position of the initial spectral line remains almost unchanged while the second line moves to lower fields similar to the one observed in $Gd_2Sn_2O_7$, so that the splitting between the two components amounts to 7-8 kOe at temperatures close to the ordering transition. As a result, the magnetic resonance spectrum of $Gd_2Ti_2O_7$ at $T = 1.3$ K consists of two lines with the gaps $\Delta_{1,2} \simeq 5$ GHz (Line I) and 26 GHz (Line II). The absorption intensity is redistributed between them so that the nearly paramagnetic Line I which is principal at the high temperatures becomes a secondary feature in the low temperature range. At frequencies below 35-40 GHz it is completely decayed into the wide band of gapped excitations corresponding to the Line II absorption and becomes unobservable in our measurements. Due to a narrowing of the two lines under magnetic field they become reliably resolved at frequencies above 90 GHz. The existence, in the vicinity of an ordering transition, of a residual mode with the gap value not exceeding 0.25 K may (i) reflect the partial disorder of the magnetic structure of $Gd_2Ti_2O_7$ below ordering proposed in Ref.10; (ii) result in the $C \propto T^2$ behaviour of the specific heat observed in $Gd_2Ti_2O_7$ well below the ordering temperature.[21]

The temperature evolution of the gaps in both compounds are illustrated in the insets of Fig. 9. The represented parameters $\nu - \gamma H_{\mathrm{res}}$ are equivalent to the gap values on the assumption that the resonance frequency increases linearly under magnetic field. These parameters start to deviate from zero at temperatures below 4-5 K and then increase linearly to the values specified above. The relation between the gaps at $T = 1.3$ K and the single-ion anisotropy constants in both compounds (anisotropy of the form $D \sum S_z^2$ determined from EPR measurements[16,17]) $\Delta/D = 1.2/0.21$ and $0.8/0.14$ are consistent with each other and roughly equal to 6.

Note that this energy exactly corresponds to the transition $|-7/2\rangle \rightarrow |-5/2\rangle$ (for $D < 0$) or $|5/2\rangle \rightarrow |7/2\rangle$ (for $D > 0$) of an isolated $S = 7/2$ magnetic ion when the magnetic field is applied along the anisotropy axis. Nevertheless, for a concentrated paramagnet at high temperatures this transition is impossible to observe separately of the transitions between other levels. As mentioned above, the resulting line should be narrowed by the exchange interaction in the vicinity of the paramagnetic position, as was observed in our experiment. In the spin-liquid phase formed at temperatures $T \ll \Theta_{CW}$ this description is not applicable, since the magnetic resonance spectrum should be related to the excitations above the collective ground state. The influence of short-range cor-

relations on the magnetic resonance in spin systems with no long-range ordering in the ground state and gapless spectrum was first reported for quasi-1D $S = 5/2$ spin chains.[22] The shift of the resonance line was attributed to the combined effect of the dipolar interaction and a single-ion anisotropy. The origin of a similar effect in pyrochlore systems is unclear and requires theoretical studies. Although the crystal field of cubic symmetry should not affect $S = 1$ excitations, the temperature and field evolution of the observed resonance absorption resembles the case of a system of triplet levels split by a single-ion anisotropy and magnetic field. On the other hand, the short-range correlations between spins on the pyrochlore-like lattice are mostly related to hexagon loops in (111)-planes,[23] so one can also suppose the observation in a spin-liquid phase of weakly dispersive modes gapped due to anisotropy and dipolar interaction. The visual absence of an orientational dependence of the spectrum might result from the high symmetry of the crystal lattice. Once the nature of the collective excitations is known precisely, a detailed analysis of this problem can be performed.

Other properties of the low temperature excitations that are significantly different from the conventional paramagnetic precession appears when the external magnetic field is applied parallel to the linear microwave field polarization. The paramagnetic precession cannot be driven in this field configuration. Therefore, the high temperature response to the microwave field is observed only at low external fields corresponding to the wing of the Lorentzian resonance line and demonstrates the rapid decrease in intensity under high fields (see Fig. 6). In contrast, the low temperature resonance modes can be excited by the longitudinal microwave field and are therefore associated with the longitudinal oscillations of the net magnetic moment. These eigen modes of spin oscillations of the exchange correlated state in the pyrochlore magnet are different from conventional spin precession. They might be analogous to the weakly dispersive optical modes of an antiferromagnetic resonance in the ordered phase. This response remains practically unchanged over the whole field range up to the saturation field and then rapidly disappears because the magnetic moment cannot be perturbed by a weak microwave field in a fully polarized phase.

In summary, the conventional isotropic paramagnetic resonance mode with $g = 2.0$ observed in $Gd_2Ti_2O_7$ and $Gd_2Sn_2O_7$ at $T \geq \Theta_{CW} \approx 10$ K gradually transforms into gapped excitations of a new type at low temperatures. Unlike conventional antiferromagnets, the gaps develop well above the transition into an ordered state over a wide temperature interval, with short-range correlations and no magnetic ordering characteristic of highly frustrated magnets. These gaps increase linearly with the magnetic field in a way that is practically independent of the field orientation with respect to the crystal axes. These properties might point to the presence of collective spin excitations split by the single-ion anisotropy.

[1] R. Moessner and J. T. Chalker, Phys. Rev. Lett. **80**, 2929 (1998).

[2] B. Canals and C. Lacroix, Phys. Rev. B **61**, 1149 (2000).

[3] N. P. Raju, M. Dion, M. J. P. Gingras, T. E. Mason, and J. E. Greedan, Phys. Rev. B **59**, 14489 (1999).

[4] A. P. Ramirez, B. S. Shastry, A. Hayashi, J. J. Krajewski, D. A. Huse, and R. J. Cava, Phys. Rev. Lett. **89**, 067202 (2002).

[5] P. Bonville, J. A. Hodges, M. Ocio, J.-P. Sanchez, P. Vulliet, S. Sosin and D. Braithwaite, J. Phys.: Condens. Matter **15**, 7777 (2003).

[6] S. E. Palmer and J. T. Chalker, Phys. Rev. B **62**, 488 (2000).

[7] A. G. del Maestro and M. J. P. Gingras, J. Phys. Condens. Matter **16**, 3339 (2004).

[8] O. Cepas, A. P. Young, and B. S. Shastry, Phys. Rev. B **72**, 184408 (2005).

[9] A. S. Wills, M. E. Zhitomirsky, B. Canals, J.-P. Sanchez, P. Bonville, P. Dalmas de Reotier, and A. Yaouanc, J. Phys.: Condens. Matter **18**, L37 (2006).

[10] J. R. Stewart, G. Ehlers, A. S. Wills, S. T. Bramwell, and J. S. Gardner, J. Phys.: Condens. Matter **16**, L321 (2004).

[11] M. E. Zhitomirsky, Phys. Rev. B **67**, 104421 (2003).

[12] S. S. Sosin, L. A. Prozorova, A. I. Smirnov, A. I. Golov, I. B. Berkutov, O. A. Petrenko, G. Balakrishnan, and M. E. Zhitomirsky, Phys. Rev. B **71**, 094413 (2005).

[13] S. S. Sosin, A. I. Smirnov, L. A. Prozorova, G. Balakrishnan, and M. E. Zhitomirsky Phys. Rev. B **73**, 212402 (2006).

[14] S. S. Sosin, A. I. Smirnov, L. A. Prozorova, O. A. Petrenko, M. E. Zhitomirsky, J.-P. Sanchez, J. Magn. Magn. Mater. **310(2)**, 1590 (2006).

[15] A. K. Hassan, L. P. Levy, C. Darie, and P. Strobel, Phys. Rev. B **67**, 214432 (2003).

[16] V. N. Glazkov, M. E. Zhitomirsky, A. I. Smirnov, H.-A. Krug von Nidda, A. Loidl, C. Marin and J.-P. Sanchez, Phys. Rev. B **72**, 020409(R) (2005).

[17] V. N. Glazkov, A. I. Smirnov, J.-P. Sanchez, A. Forget, D. Colson and P. Bonville, J. Phys.: Condens. Matter **18**, 2285 (2006).

[18] G. Balakrishnan, O. A. Petrenko, M. R. Lees, and D. McK. Paul, J. Phys. Condens. Matter **10**, L723 (1998).

[19] O. A. Petrenko, M. R. Lees, G. Balakrishnan, D. McK. Paul, Phys. Rev. B **70**, 012402 (2004).

[20] Y. Narumi, A. Kikkawa, K. Katsumata, Z. Honda, M. Hagiwara, and K. Kindo, AIP Conf. Proc. **850**, 1113 (2006).

[21] A. Yaouanc, P. Dalmas de Reotier, V. Glazkov, C. Marin, P. Bonville, J. A. Hodges, P. C. M. Gubbens, S. Sakarya, and C. Baines, Phys. Rev. Lett. **95**, 047203 (2005).

[22] K. Nagata, Y. Tazuke, J. Phys. Soc. Japan **32**, 337 (1972).

[23] S.-H. Lee, C. Broholm, W. Ratcliff, G. Gasparovic, Q. Huang, T. H. Kim, and S.-W. Cheong, Nature **418**, 856 (2002).